19th International Conference
ENGINEERING MECHANICS 2013
Svratka, Czech Republic, May 13 – 16, 2013

COMPARISON OF NUMERICAL METHODS FOR UNCERTAINTY QUANTIFICATION

E. Janouchová, A. Kučerová, J. Sýkora [1]

Summary:
An extensive development of efficient methods for stochastic modelling enabled uncertainty propagation through complex models. In this contribution, we present a review and comparison of several approaches such as stochastic Galerkin method, stochastic collocation method or polynomial regression based on Latin Hypercube Sampling. The advantages and disadvantages of these methods are demonstrated within the comparison with the traditional Monte Carlo method on a simple illustrative example of a frame structure.

1. Introduction

There are many important factors limiting the service life of buildings. An appropriate reliability analysis needs to take account uncertainties in the environmental conditions as well as in structural properties. Thanks to the growth of powerful computing resources and technology, recently developed procedures in the field of stochastic mechanics have become applicable to realistic engineering systems. Methods quantifying uncertainties can be classified into two groups: (i) reliability analysis methods, such as the first- and second-order reliability method (FORM/SORM (Ditlevsen, 1996)) computing the probability of failure related to limit states; (ii) the higher moment analysis focused on estimation of the higher-order statistical moments of structural response as stochastic finite element methods (SFEM), see (Matthies, 2007; Stefanou, 2009) for a review. SFEM is a powerful tool in computational stochastic mechanics extending the classical deterministic finite element method (FEM) to the stochastic framework involving finite elements whose properties are random (Ghanem, 1991).

In this contribution we concentrate on the SFEM based on polynomial chaos expansion (PCE) used for approximation of the model response in the stochastic space. Uncertainty in the model output can be then quantified using Markov chain Monte Carlo method employed for sampling model parameters and evaluating the PCE instead of full numerical model. The efficiency of SFEM thus depends on computational requirements of the PCE construction and its consequent accuracy.

There are several methods for construction of PCE-based approximation of a model response: stochastic Galerkin method (Babuska et al., 2004; Matthies and Keese, 2005), stochastic collocation methods (Babuska et al., 2007; Xiu, 2009) and linear regression (Blatman and

[1] Bc. Eliška Janouchová, Ing. Anna Kučerová, Ph.D., Ing. Jan Sýkora, Ph.D., Faculty of Civil Engineering, Czech Technical University in Prague, Thákurova 7/2077, 166 29 Prague 6, tel. +420 224 35 53 26, e-mail eliska.janouchova@fsv.cvut.cz, anicka@cml.fsv.cvut.cz, jan.sykora.1@fsv.cvut.cz

Sudret, 2010). The principal differences among these methods are follows. Stochastic Galerkin method is purely deterministic, but leads to solution of large system of equation and needs an intrusive modification of the numerical model itself. Stochastic collocation methods is also a deterministic method, does not require intrusive modification of a model, but uses a set of model simulations on a sparse grid constructed for a chosen level of accuracy. The computation of PCE coefficients is based on explicit formula. The linear regression is based again on a set of model simulations performed for a stochastic design of experiments, usually obtained by Latin Hypercube Sampling. The PCE coefficients are then obtained by regression of a model results at the design points, which leads to a solution of a system of equations. The aim of this paper is to compare these methods in terms of computational requirements and resulting accuracy on a simple illustrative example of a frame structure.

2. Motivation

In order to demonstrate a performance of the methods on an engineering structure, we have chosen a simple frame presented in (Marek et al., 2003). The geometry, load distribution and supports of the frame are shown in Figure 1.

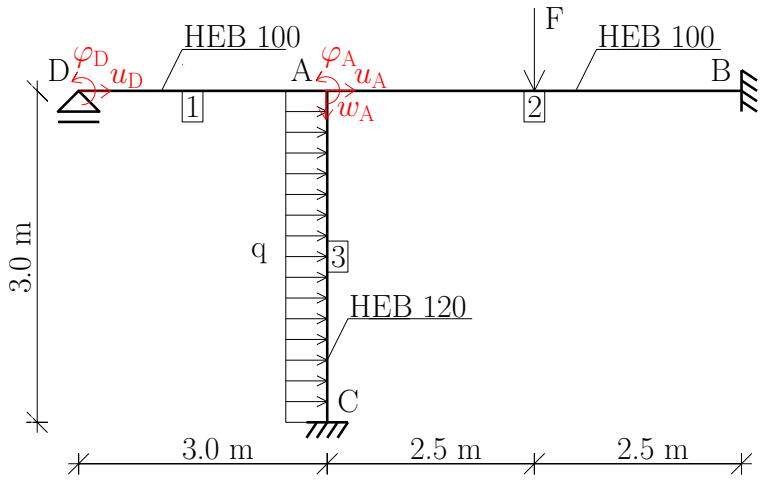

Figure 1: Scheme of a frame structure.

The geometrical parameters of particular beams are considered as uncertain with a given nominal value and uncertain variation defined by a prescribed histogram given in (Marek et al., 2003) and depicted in Figure 2. Particular nominal values, corresponding random variables and types of histograms are listed in Table 1. The prescribed loading are linear combinations of dead load, long-lasting load and short-lasting load given as:

$$q = D_1 D_{\sigma 1} + S_1 S_{\sigma 1} + L_1 L_{\sigma 1} \ [\mathrm{kN/m}], \quad (1)$$

$$F = D_2 D_{\sigma 2} + S_2 S_{\sigma 2} + L_2 L_{\sigma 2} \ [\mathrm{kN}], \quad (2)$$

where particular loads are statistically independent and described by random variables with extreme values and variations defined by histograms given in Table 2 and depicted in Figure 2.

The maximal internal forces will appear in the column at support C and can be computed from the displacement and rotation of the joint A. The unknown displacements $\boldsymbol{r}$ can be for

Table 1: Geometrical data and variations

Geometrical data	Nominal value	Variable	Histogram
Moment of inertia	$I_1 = 449.5\ \mathrm{cm}^4$	$I_{\sigma 1}$	N1-05
Moment of inertia	$I_2 = 449.5\ \mathrm{cm}^4$	$I_{\sigma 2}$	N1-05
Moment of inertia	$I_3 = 864.4\ \mathrm{cm}^4$	$I_{\sigma 3}$	N1-05
Length	$l_1 = 3$ m	l_σ	N1-01
Length	$l_2 = 5$ m	l_σ	N1-01
Length	$l_3 = 4$ m	l_σ	N1-01

Table 2: Loading and variations

Load	Extreme Value	Variable	Histogram
Dead load	$D_1 = 11$ kN/m	$D_{\sigma 1}$	DEAD2
Short-lasting load	$S_1 = 9$ kN/m	$S_{\sigma 1}$	SHORT1
Long-lasting load	$L_1 = 5.5$ kN/m	$L_{\sigma 1}$	LONG1
Dead load	$D_2 = 3.5$ kN	$D_{\sigma 2}$	DEAD2
Short-lasting load	$S_2 = 2.2$ kN	$S_{\sigma 2}$	SHORT1
Long-lasting load	$L_2 = 1.7$ kN	$L_{\sigma 2}$	LONG1

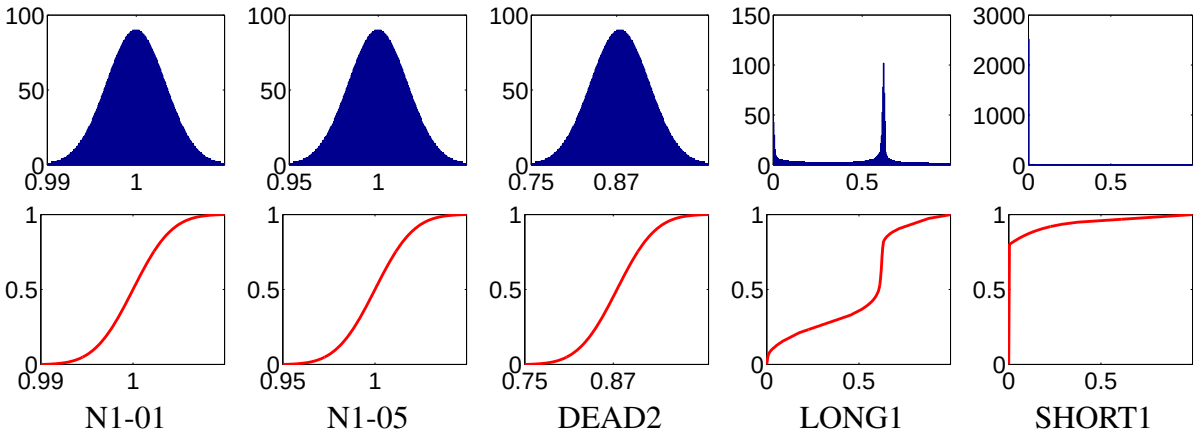

Figure 2: Histograms of uncertain parameters and corresponding cumulative density functions.

linear elastic behaviour considered here computed by the finite element method or displacement method, which are very well-known. Hence, we start directly with the latter one from discretised form of equilibrium equations:

$$\mathbf{K}\boldsymbol{r} = \boldsymbol{f}\,, \tag{3}$$

which – after applying the boundary conditions – takes the following particular form:

$$\begin{bmatrix} \frac{A_1 I_{\sigma 1}}{12 l_1} & 0 & -\frac{A_1 I_{\sigma 1}}{12 l_1} & 0 & 0 \\ 0 & \frac{I_1 I_{\sigma 1}}{3 l_1} & 0 & \frac{I_1 I_{\sigma 1}}{2 l_1^2 l_\sigma} & \frac{I_1 I_{\sigma 1}}{6 l_1} \\ -\frac{A_1 I_{\sigma 1}}{12 l_1} & 0 & \frac{A_1 I_{\sigma 1}}{12 l_1} + \frac{A_2 I_{\sigma 2}}{12 l_2} + \frac{I_3 I_{\sigma 3}}{l_3^2 l_\sigma^2} & 0 & \frac{I_3 I_{\sigma 3}}{2 l_3^2 l_\sigma} \\ 0 & \frac{I_1 I_{\sigma 1}}{2 l_1^2 l_\sigma} & 0 & \frac{I_1 I_{\sigma 1}}{l_1^3 l_\sigma^2} + \frac{I_2 I_{\sigma 2}}{l_2^3 l_\sigma^2} + \frac{A_3 I_{\sigma 3}}{12 l_3} & \frac{I_1 I_{\sigma 1}}{2 l_1^2 l_\sigma} - \frac{I_2 I_{\sigma 2}}{2 l_2^2 l_\sigma} \\ 0 & \frac{I_1 I_{\sigma 1}}{6 l_1} & \frac{I_3 I_{\sigma 3}}{2 l_3^2 l_\sigma} & \frac{I_1 I_{\sigma 1}}{2 l_1^2 l_\sigma} - \frac{I_2 I_{\sigma 2}}{2 l_2^2 l_\sigma} & \frac{I_1 I_{\sigma 1}}{3 l_1} + \frac{I_2 I_{\sigma 2}}{3 l_2} + \frac{I_3 I_{\sigma 3}}{3 l_3} \end{bmatrix} \cdot$$

$$\cdot \frac{12E}{l_\sigma} \cdot \begin{pmatrix} u_{\mathrm{D}} \\ \varphi_{\mathrm{D}} \\ u_{\mathrm{A}} \\ w_{\mathrm{A}} \\ \varphi_{\mathrm{A}} \end{pmatrix} = \begin{pmatrix} 0 \\ 0 \\ \frac{(D_1 D_{\sigma 1} + S_1 S_{\sigma 1} + L_1 L_{\sigma 1}) l_3 l_\sigma}{2} \\ \frac{D_2 D_{\sigma 2} + S_2 S_{\sigma 2} + L_2 L_{\sigma 2}}{2} \\ -\frac{(D_2 D_{\sigma 2} + S_2 S_{\sigma 2} + L_2 L_{\sigma 2}) l_2 l_\sigma}{8} + \frac{(D_1 D_{\sigma 1} + S_1 S_{\sigma 1} + L_1 L_{\sigma 1})(l_3 l_\sigma)^3}{12} \end{pmatrix}. \quad (4)$$

3. Polynomial chaos expansion

In order to accelerate the sampling procedure in uncertainty propagation process, the evaluations of a numerical model including solutions of Eq. (3) can be replaced by evaluations of a model surrogate. In particular, we search for an approximation of the response $\boldsymbol{r}$ by polynomial chaos expansion (PCE) (Matthies, 2007; Stefanou, 2009). PCE can be used to approximate the response with respect to probability distribution of the random variables. The approximation of the response is then weighted according to the probability distribution of variables i.e. the approximation is more precise in regions with higher probability. The convergence of the approximation error with the increasing number of polynomial terms is optimal in case of orthogonal polynomials of a special type corresponding to the probability distribution of the underlying variables (Xiu and Karniadakis, 2002). For example, Hermite polynomials are associated with the Gaussian distribution, Legendre polynomials with the uniform distribution and so on.

In the example described in the previous section, all the random variables are listed in Tables 1 and 2. Let us simplify the notation and denote them as m_i, $\boldsymbol{m} = (\dots, m_i, \dots)^{\mathrm{T}} = (I_{\sigma 1}, I_{\sigma 2}, I_{\sigma 3}, l_\sigma, D_{\sigma 1}, S_{\sigma 1}, L_{\sigma 1}, D_{\sigma 2}, S_{\sigma 2}, L_{\sigma 2})^{\mathrm{T}}$. Since none of these variables has a continuous probability density function (PDF), but their distribution is described by discrete histograms, we introduce new standard random variables $\boldsymbol{\xi} = (\dots, \xi_i, \dots)^{\mathrm{T}})$ with a continuous PDF. The variables m_i can be then expressed by transformation functions t_{jk} of variables ξ_i according to the given histogram j and type k of the ξ_i distribution, i.e.

$$m_i = t_{jk}(\xi_i)\,. \quad (5)$$

For case of discrete histograms, the transformation functions are non-smooth. Particular examples of transformation functions will be discussed in Section 4.

Once we have expressed the model variables $\boldsymbol{m}$ as functions of standard variables $\boldsymbol{\xi}$, also the model response becomes a function of these variables. This function can be thus approximated by the PCE of a type corresponding to the type of $\boldsymbol{\xi}$ distribution, i.e.

$$\tilde{\boldsymbol{r}}(\boldsymbol{\xi}) = \sum_{\alpha} \boldsymbol{\beta}_\alpha \psi_\alpha(\boldsymbol{\xi}), \quad (6)$$

where $\boldsymbol{\beta}_\alpha$ is a vector of PC coefficients $\beta_{\alpha,i}$ corresponding to a particular component of system response r_i. $\psi_\alpha(\boldsymbol{\xi})$ are multivariate polynomials. The expansion (6) is usually truncated to the limited number of terms n_β, which is very often related to the number of random variables n_ξ and to the maximal degree of polynomials n_p according to the relation $n_\beta = \frac{(n_\mathrm{p}+n_\xi)!}{n_\mathrm{p}!n_\xi!}$.

3.1. Linear regression

A very general method of computing PC coefficients in Eq. (6) is a well-known linear regression (Blatman and Sudret, 2010). The underlying assumption of linear regression is that the surrogate $\tilde{\boldsymbol{r}}$ is a linear combination of the parameters $\boldsymbol{\beta}$, but does not have to be linear in the independent variables $\boldsymbol{\xi}$. The application is based on the three following steps: (i) preparation of data $\boldsymbol{\Xi} \in \mathbb{R}^{n_\xi \times n_\mathrm{d}}$ which are obtained as n_d samples of parameter vector $\boldsymbol{\xi}_i$ (ii) evaluation of the model for samples $\boldsymbol{\xi}_i$ resulting in response samples $\boldsymbol{r}_i$ organised into the matrix $\mathbf{R} \in \mathbb{R}^{n_\mathrm{r} \times n_\mathrm{d}}$, where n_r is a number of response components and (iii) computation of PC coefficients $\boldsymbol{\beta}_\alpha$ organised into the matrix $\mathbf{B} \in \mathbb{R}^{n_\mathrm{r} \times n_\beta}$ using e.g. the ordinary least square method (OLS).

Since the most time-consuming part of this method consists in evaluations of the model for samples of random variables, the choice of these samples represents a crucial task with the highest impact on the computational time requirements. The simplest way is to choose the samples by Monte Carlo method, i.e. to draw them randomly from the prescribed probability distribution. However, the accuracy of the resulting surrogate depends on a quality, how the samples cover the defined domain. The same quality can be achieved by smaller number of samples when drawn according to some stratified procedure called design of experiments (DoE). Latin hypercube sampling (LHS) is a well-known DoE able to respect the prescribed probability distributions. There exist also more enhanced way of optimising the LHS (see e.g. (Janouchová and Kučerová, 2013)), but these are not subject of the present work and the simplest version of unoptimised LHS is employed. Each computation of a response sample $\boldsymbol{r}_i$ then includes the evaluation of the transformations (5) and the evaluation of the model (3).

The computation of the PC coefficients $\mathbf{B}$ starts by evaluation of all the polynomial terms ψ_α for all the samples $\boldsymbol{\xi}_i$ and saving them in the matrix $\mathbf{Z} \in \mathbb{R}^{n_\mathrm{d} \times n_\beta}$. The ordinary least square method then leads to

$$\mathbf{Z}^\mathrm{T}\mathbf{Z}\mathbf{B}^\mathrm{T} = \mathbf{Z}^\mathrm{T}\mathbf{R}^\mathrm{T} \tag{7}$$

which is a linear system of n_β equations.

3.2. Stochastic collocation

Stochastic collocation method is based on an explicit expression of the PC coefficients:

$$\beta_{\alpha,i} = \int r_i(\boldsymbol{\xi})\psi_\alpha(\boldsymbol{\xi})\,\mathrm{d}\mathbb{P}(\boldsymbol{\xi})\,, \tag{8}$$

which can be solved numerically using an appropriate integration rule (quadrature) on $\mathbb{R}^{n_\xi}$. Equation (9) then becomes

$$\beta_{\alpha,i} = \sum_{j=1}^{n_\mathrm{d}} r_i(\boldsymbol{\xi}_j)\psi_\alpha(\boldsymbol{\xi}_j)w_j\,, \tag{9}$$

where $\boldsymbol{\xi}_j$ stands for an integration node and w_j is a corresponding weight. Here we employ versions of the Smolyak quadrature rule, in particular quadratures with the Gaussian rules as basis

for uniform (GQU) and normal (GQN) distributions and nested Kronrod-Patterson quadrature rules for uniform (KPU) and normal (KPN) distributions, see Heiss and Winschel (2008).

It is clear that the stochastic collocation method is similar to linear regression, because in both cases the most computational effort is needed for evaluation of a set of model simulations. The principal difference can be seen in sample generation, where stochastic collocation method uses a preoptimised sparse grids while the linear regression is based on stochastic LHS.

3.3. Stochastic Galerkin

Stochastic Galerkin method is principally different to the previous ones, which are based on a set of independent model simulations. Stochastic Galerkin method is an intrusive method, i.e. it requires reformulation ofthe governing equations of the model (3). To this purpose, we rewrite Equation (6) in using matrix notation

$$\tilde{\boldsymbol{r}}(\xi) = (\mathbf{I} \otimes \boldsymbol{\psi}(\boldsymbol{\xi}))\boldsymbol{\beta}, \tag{10}$$

where $\mathbf{I} \in \mathbb{R}^{n_\mathrm{r} \times n_\mathrm{r}}$ is the unity matrix, $\otimes$ is the Kronecker product, $\boldsymbol{\psi}(\boldsymbol{\xi})$ is a n_β-dimensional vector of polynomials and $\boldsymbol{\beta}$ is a $(n_\beta \cdot n_\mathrm{r})$-dimensional vector of PC coefficients organised here as $\boldsymbol{\beta} = (\dots, \boldsymbol{\beta}_i, \dots)^\mathrm{T}$, where $\boldsymbol{\beta}_i$ consists of PC coefficients corresponding to i-th response component.

Substituting the model response $\boldsymbol{r}$ in Equation (3) by its PC approximation $\tilde{\boldsymbol{r}}$ given in Equation (10) and applying Galerkin conditions, we obtain

$$\int \boldsymbol{\psi}(\boldsymbol{\xi}) \otimes \mathbf{K}(\boldsymbol{\xi}) \otimes \boldsymbol{\psi}^\mathrm{T}(\boldsymbol{\xi}) \,\mathrm{d}\mathbb{P}(\boldsymbol{\xi}) \cdot \boldsymbol{\beta} = \int \boldsymbol{\psi}(\boldsymbol{\xi}) \otimes \boldsymbol{f}(\boldsymbol{\xi}) \,\mathrm{d}\mathbb{P}(\boldsymbol{\xi}) \,, \tag{11}$$

which is a linear system of $(n_\beta \cdot n_\mathrm{r})$ equations. The integration can be done numerically or analytically. The analytical solution is available e.g. when all terms in the stiffness matrix and in the loading vector are polynomials with respect to $\boldsymbol{\xi}$. In such a case, the method is called *fully intrusive*. In our particular example, we can multiply the governing Equation (4) by l_σ^3 so as to obtain polynomials in terms of model parameters $\boldsymbol{m}$. However, we will not obtain polynomials in terms of $\boldsymbol{\xi}$ due to non-smooth transformations (5) produced by discrete nature of histograms prescribed to $\boldsymbol{m}$. Hence, in such a case, a numerical integration leading to *semi-intrusive* Galerkin method is inevitable.

4. Results

The goal of the presented work is to compare the described methods for approximating the model response and accelerating the Monte Carlo (MC) sampling performed for estimation of probability distribution of displacements u_A, w_A and φ_A.

4.1. Hermite polynomials

We start by assuming $\boldsymbol{\xi}$ as standard Gaussian variables and thus we employ Hermite polynomials for model surrogate. The reference estimation of mean μ and standard deviation σ of particular displacements is obtained by MC sampling with 10^7 samples. Table 3 shows the required computational time and relative errors in predictions for linear regression and stochastic

collocation method for four polynomial degrees p. The relative errors in the mean prediction are obtained as $\varepsilon_\mu = \frac{|\mu_{\mathrm{PCE}} - \mu_{\mathrm{MC}}|}{\mu_{\mathrm{MC}}}$, where μ_{MC} stands for the mean estimated by the MC method and and μ_{PCE} stands for the mean obtained using a chosen surrogate. The relative errors in predictions of standard deviations are obtained in a same way.

Table 3: Time requirements and errors in predicting response mean and standard deviation in case of **prescribed histograms** for model parameters $\boldsymbol{m}$.

Method	n_{d}	p	**Time** [s]	u_{A}[mm]		w_{A}[mm]		φ_{A}[mrad]	
				μ	σ	μ	σ	μ	σ
MC	10^7	–	22191	0.21	0.03	0.01	0.00	4.09	0.79
				ε_μ [%]	ε_σ [%]	ε_μ [%]	ε_σ [%]	ε_μ [%]	ε_σ [%]
LHS	21	1	133	0.09	28.32	0.62	44.07	0.02	27.59
	201	2	622	0.02	0.36	0.40	1.02	0.06	0.05
	1201	3	2687	0.01	0.13	0.09	1.77	0.03	0.12
	5301	4	8696	0.04	0.21	0.01	0.78	0.04	0.23
KPN	21	1	166	4.81	9.34	4.25	8.42	4.89	9.37
	201	2	811	4.81	5.50	4.25	4.30	4.89	5.48
	1201	3	2648	2.25	7.32	1.97	3.69	2.30	5.14
	5301	4	8721	0.31	11.32	0.29	6.15	0.31	7.91
GQN	21	1	132	6.68	22.99	6.07	15.51	6.78	23.01
	221	2	623	4.81	73.94	4.25	50.99	4.90	58.18
	1581	3	2706	3.12	59.65	2.81	37.00	3.17	46.84
	8761	4	8698	1.13	187.85	1.10	129.41	1.14	147.77

The results show very good predictions obtained by linear regression, while stochastic collocation based on KPN rules leads to considerable errors in prediction of standard deviations and GQN rules seems even diverging. However, when looking at the whole probability density functions obtained for u_A depicted in Figure 3, even the prediction obtained by linear regression is not satisfactory.

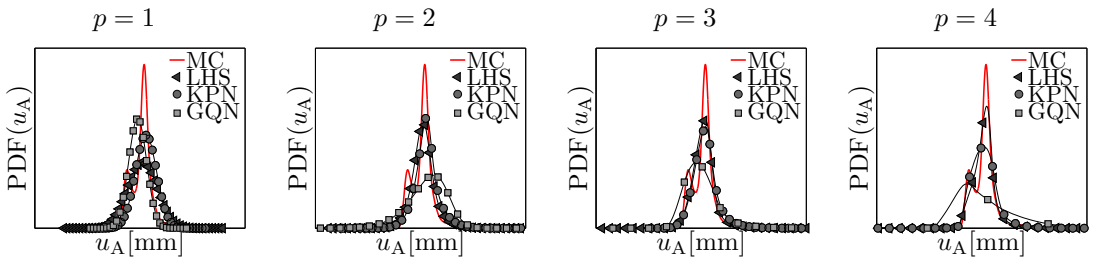

Figure 3: Probability density functions of displacement u_A in case of **prescribed histograms** for model parameters $\boldsymbol{m}$.

The reason for such unsatisfactory results is probably highly nonlinear transformation (5) for parameters with prescribed histograms LONG1 and SHORT1, as shown in Figure 4. In order to test this assumptions, we have replaced these two prescribed histograms by the new ones more close to normal distribution, see Figure 5. New errors in predicting mean and standard deviations are listed in Table 4.

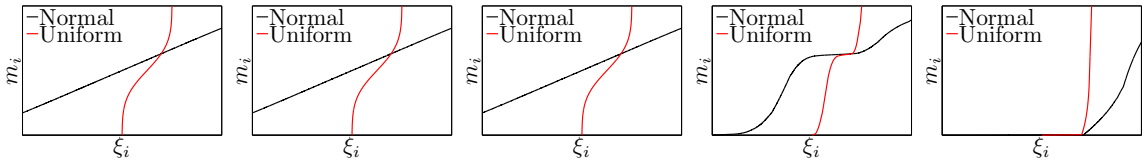

N1-01 N1-05 DEAD2 LONG1 SHORT1

Figure 4: Transformation relations for prescribed histograms.

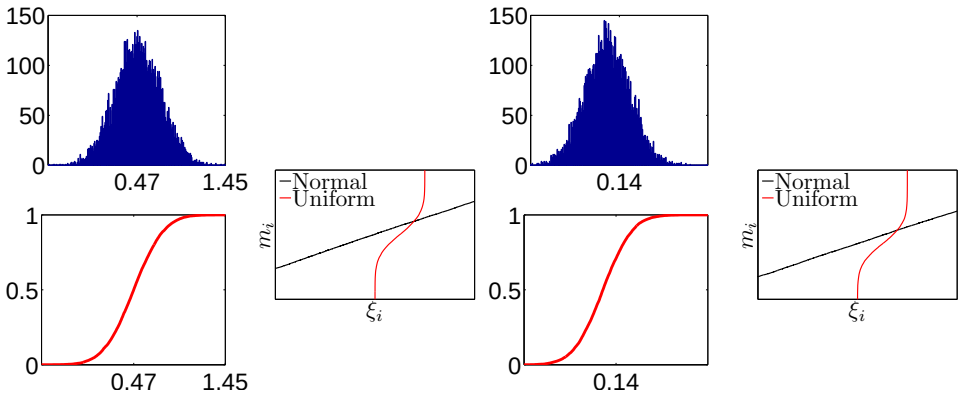

LONG1new SHORT1new

Figure 5: New histograms of model parameters with corresponding cumulative density functions and transformation relations.

Table 4: Time requirements and errors in predicting response mean and standard deviation in case of **new histograms** for model parameters $\boldsymbol{m}$.

Method	n_d	**p**	**Time** [s]	u_A[mm]		w_A[mm]		φ_A[mrad]	
				μ	σ	μ	σ	μ	σ
MC	10^7	–	21874	0.21	0.03	0.01	0.00	4.06	0.79
				ε_μ [%]	ε_σ [%]	ε_μ [%]	ε_σ [%]	ε_μ [%]	ε_σ [%]
LHS	21	1	158	0.03	0.85	0.02	0.54	0.04	1.17
	201	2	673	0.00	0.06	0.03	0.22	0.01	0.08
	1201	3	2736	0.01	0.03	0.01	0.06	0.01	0.02
	5301	4	8770	0.00	0.04	0.00	0.01	0.01	0.03
KPN	21	1	132	0.06	0.12	0.05	0.06	0.06	0.11
	201	2	654	0.06	0.08	0.05	0.01	0.06	0.08
	1201	3	2768	0.02	0.26	0.01	0.19	0.02	0.26
	5301	4	8978	0.00	0.13	0.01	0.13	0.00	0.14
GQN	21	1	132	0.07	0.21	0.06	0.20	0.07	0.19
	221	2	668	0.06	0.06	0.05	0.00	0.06	0.07
	1581	3	2770	0.03	0.48	0.03	0.29	0.03	0.48
	8761	4	8988	0.00	0.21	0.00	0.20	0.00	0.20

One can see that the replacement of the two histograms led to a significant improvement of the results achieved by all the methods, but we can also notice that the GQN based collocation provide very good worse than the other methods and also the difficulties with convergence. On

the other hand, linear regression gives the worst prediction for 1^{st} order polynomials, but these are improved by very fast convergence.

The same improvement can be seen also in prediction of the whole probability density function depicted in Figure 6.

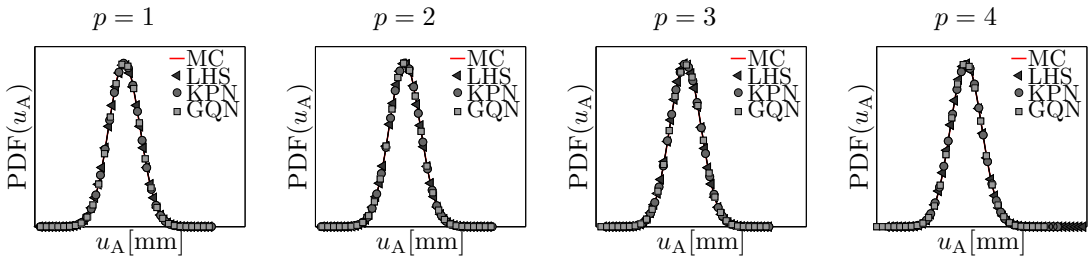

Figure 6: Probability density functions of displacement u_A in case of **new histograms** for model parameters $\boldsymbol{m}$.

In order to investigate the performance of fully intrusive stochastic Galerkin method, we have changed the prescribed distributions for model parameters once more. This time, we assume all the parameters to be normally distributed with the original values of mean and standard deviation. In such a case, the transformation (5) becomes the 1^{st} order polynomial and hence, analytical integration is available. Figure 7 shows the functional dependence of displacement u_A for described types of probability distribution prescribed to model parameters. Figure 7a shows that the relation between u_A and model parameters $\boldsymbol{m}$ is linear, while the high nonlinearity appears in the relation to standard variables $\boldsymbol{\xi}$ in case of prescribed histograms, see Figure 7b. Replacement of the two histograms LONG1 and SHORT1 by the new ones more similar to normal distributions leads to almost linear $u_A - \boldsymbol{\xi}$ relation namely in the high probability region, see Figure 7c. Finally, prescription of the normal distribution to model parameters provides the linear $u_A - \boldsymbol{\xi}$ relation as shown in Figure 7d.

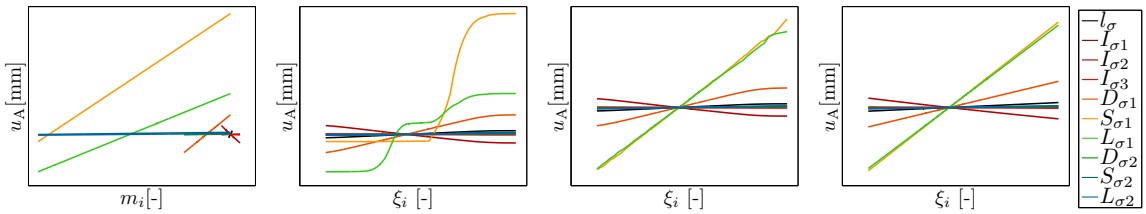

Figure 7: Functional dependence of displacement u_A on model parameters $\boldsymbol{m}$ (a), on standard variables $\boldsymbol{\xi}$ in case of prescribed histograms (b), in case of new histograms (c) and in case of normal distribution (d).

The errors in prediction of mean, standard deviation and whole PDF are shown in Table 5 and Figure 8 including results obtained by fully intrusive stochastic Galerkin method. The results proof that the $u_A - \boldsymbol{\xi}$ relation is now linear and thus the 1^{st} order polynomials are sufficient for an excellent surrogate and the differences among the particular methods are here negligible in terms of accuracy as well as the time requirements.

Table 5: Time requirements and errors in predicting response mean and standard deviation in case of **normal distribution** for model parameters $\boldsymbol{m}$.

Method	n_{d}	**p**	**Time** [s]	u_{A}[mm]		w_{A}[mm]		φ_{A}[mrad]	
				μ	σ	μ	σ	μ	σ
MC	10^7	–	3692	0.207	0.033	0.009	0.002	4.090	0.795
				ε_μ [%]	ε_σ [%]	ε_μ [%]	ε_σ [%]	ε_μ [%]	ε_σ [%]
LHS	21	1	132	$4 \cdot 10^{-2}$	$3 \cdot 10^{-1}$	$5 \cdot 10^{-2}$	$5 \cdot 10^{-1}$	$6 \cdot 10^{-2}$	$6 \cdot 10^{-1}$
	201	2	618	$4 \cdot 10^{-5}$	$7 \cdot 10^{-3}$	$1 \cdot 10^{-3}$	$1 \cdot 10^{-3}$	$3 \cdot 10^{-4}$	$3 \cdot 10^{-3}$
	1201	3	2702	$4 \cdot 10^{-6}$	$4 \cdot 10^{-5}$	$5 \cdot 10^{-6}$	$2 \cdot 10^{-5}$	$5 \cdot 10^{-7}$	$4 \cdot 10^{-6}$
	5301	4	8680	$2 \cdot 10^{-7}$	$1 \cdot 10^{-6}$	$2 \cdot 10^{-7}$	$4 \cdot 10^{-7}$	$4 \cdot 10^{-8}$	$2 \cdot 10^{-8}$
KPN	21	1	135	$2 \cdot 10^{-5}$	$4 \cdot 10^{-2}$	$2 \cdot 10^{-4}$	$6 \cdot 10^{-2}$	$6 \cdot 10^{-5}$	$2 \cdot 10^{-2}$
	201	2	618	$4 \cdot 10^{-6}$	$1 \cdot 10^{-5}$	$2 \cdot 10^{-6}$	$3 \cdot 10^{-5}$	$3 \cdot 10^{-6}$	$2 \cdot 10^{-5}$
	1201	3	2725	$3 \cdot 10^{-8}$	$5 \cdot 10^{-7}$	$2 \cdot 10^{-7}$	$2 \cdot 10^{-7}$	$2 \cdot 10^{-8}$	$2 \cdot 10^{-7}$
	5301	4	8662	$2 \cdot 10^{-11}$	$2 \cdot 10^{-8}$	$4 \cdot 10^{-9}$	$2 \cdot 10^{-9}$	$4 \cdot 10^{-10}$	$1 \cdot 10^{-9}$
GQN	21	1	132	$3 \cdot 10^{-5}$	$4 \cdot 10^{-2}$	$2 \cdot 10^{-4}$	$6 \cdot 10^{-2}$	$6 \cdot 10^{-5}$	$2 \cdot 10^{-2}$
	221	2	620	$4 \cdot 10^{-6}$	$4 \cdot 10^{-5}$	$2 \cdot 10^{-6}$	$7 \cdot 10^{-5}$	$3 \cdot 10^{-6}$	$3 \cdot 10^{-5}$
	1581	3	2757	$3 \cdot 10^{-8}$	$5 \cdot 10^{-7}$	$1 \cdot 10^{-7}$	$3 \cdot 10^{-7}$	$2 \cdot 10^{-8}$	$2 \cdot 10^{-7}$
	8761	4	8701	$9 \cdot 10^{-11}$	$2 \cdot 10^{-8}$	$4 \cdot 10^{-9}$	$3 \cdot 10^{-9}$	$4 \cdot 10^{-10}$	$1 \cdot 10^{-9}$
GM	–	1	133	$3 \cdot 10^{-5}$	$4 \cdot 10^{-2}$	$4 \cdot 10^{-3}$	$6 \cdot 10^{-2}$	$6 \cdot 10^{-5}$	$1 \cdot 10^{-2}$
	–	2	620	$4 \cdot 10^{-6}$	$4 \cdot 10^{-5}$	$4 \cdot 10^{-3}$	$1 \cdot 10^{-1}$	$3 \cdot 10^{-6}$	$4 \cdot 10^{-6}$
	–	3	2673	$5 \cdot 10^{-8}$	$3 \cdot 10^{-6}$	$4 \cdot 10^{-3}$	$1 \cdot 10^{-1}$	$5 \cdot 10^{-7}$	$2 \cdot 10^{-5}$
	–	4	8704	$8 \cdot 10^{-8}$	$2 \cdot 10^{-6}$	$4 \cdot 10^{-3}$	$1 \cdot 10^{-1}$	$4 \cdot 10^{-7}$	$2 \cdot 10^{-5}$

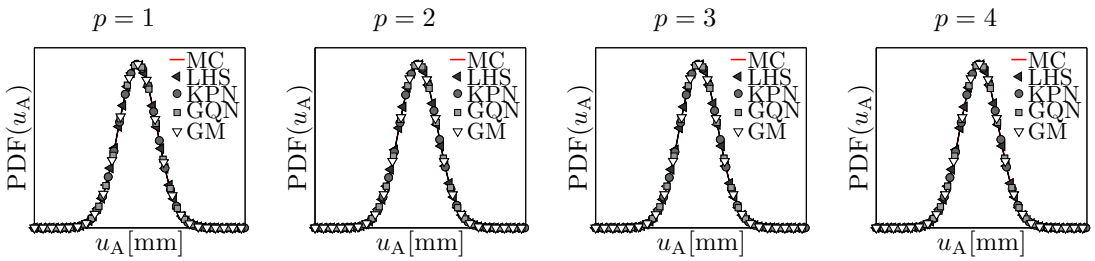

Figure 8: Probability density functions of displacement u_A in case of **normal distribution** for model parameters $\boldsymbol{m}$.

4.2. Legendre polynomials

In order to complete the presented comparative study, we also tested the usage of uniformly distribution standard variables $\boldsymbol{\xi}$ accompanied by the surrogate based on Legendre polynomials. Here again we have tried two situations, first with the prescribed histograms and second with the prescribed uniform distribution. The results presented in Table 6 and Figure 9 manifest overall worse behaviour of the Legendre surrogates.

Table 6: Time requirements and errors in predicting response mean and standard deviation using the surrogate based on Legendre polynomials.

	Method	n_d	p	Time [s]	u_A[mm]		w_A[mm]		φ_A[mrad]	
					μ	σ	μ	σ	μ	σ
Uniform	**MC**	10^7	–	3754	0.27	0.05	0.01	0.00	5.46	1.20
					ε_μ [%]	ε_σ [%]	ε_μ [%]	ε_σ [%]	ε_μ [%]	ε_σ [%]
	LHS	23	1	132	0.02	0.57	0.26	1.19	36.33	71.13
		243	2	619	0.70	0.12	0.49	0.08	36.15	71.75
		1607	3	2703	0.67	0.60	0.57	0.63	36.17	71.98
Histogram	**MC**	10^7	–	21207	0.21	0.03	0.01	0.00	4.09	0.79
					ε_μ [%]	ε_σ [%]	ε_μ [%]	ε_σ [%]	ε_μ [%]	ε_σ [%]
	LHS	23	1	132	0.89	33.76	0.85	11.24	29.40	138.19
		243	2	623	15.71	33.35	18.95	28.56	33.00	297.79
		1607	3	2692	79.24	1194.17	50.22	979.51	532.55	2042.39

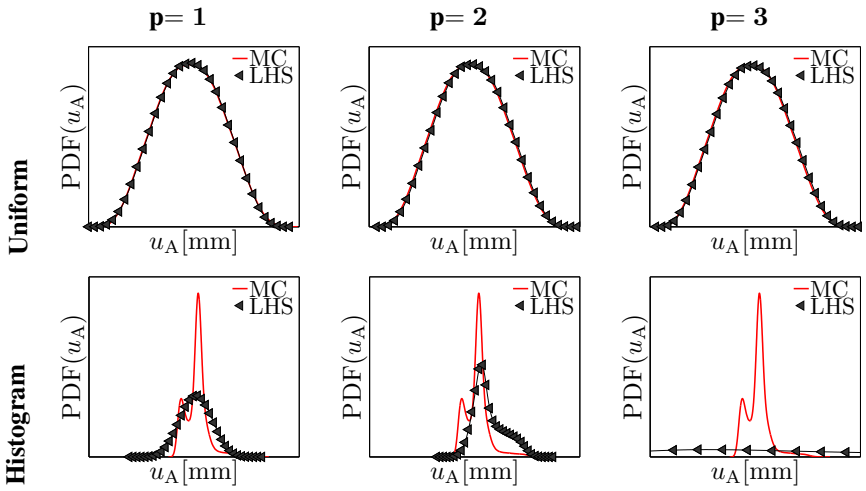

Figure 9: Probability density functions of displacement u_A obtained using the surrogate based on Legendre polynomials.

5. Conclusion

The presented paper presents a review and comparison of three methods for construction of a polynomial chaos-based surrogate of a numerical model under the assumption of random model parameters. In particular, the investigated methods are stochastic Galerkin method, stochastic collocation method and polynomial regression based on Latin Hypercube Sampling. Particular features of these methods are discussed throughout the paper. The quality of obtained surrogates in terms of accuracy as well as the time requirements are demonstrated within the comparison with the traditional Monte Carlo method on a simple illustrative example of a frame structure.

6. Acknowledgment

This outcome has been achieved with the financial support of the Czech Science Foundation, projects No. 105/11/0411 and 105/12/1146, and Grant Agency of the Czech Technical University in Prague, grant No. SGS OHK1-042/13.

7. References

Babuska, I. & Tempone, R. & Zouraris, G. E. 2004: Galerkin Finite Element Approximations of Stochastic Elliptic Partial Differential Equations. *SIAM Journal on Numerical Analysis* 42(2), 800–825.

Babuska, I. & Nobile F. & Tempone, R. 2007: A Stochastic Collocation Method for Elliptic Partial Differential Equations with Random Input Data. *SIAM Journal on Numerical Analysis* 45(3), 1005–1034.

Blatman, G. & Sudret, B. 2010: An adaptive algorithm to build up sparse polynomial chaos expansions for stochastic finite element analysis *Probabilistic Engineering Mechanics* 25(2), 183–197.

Ditlevsen, O. & Madsen, H. O. 1996: *Structural Reliability Methods*, John Wiley & Sons Ltd, Chichester, England.

Ghanem, R. G. & Spanos, P. D. 1991 *Stochastic finite elements: A spectral approach*, Springer-Verlag New York, Inc.

Heiss, F. & Winschel, V. 2008: Likelihood approximation by numerical integration on sparse grids. *Journal of Econometrics* 144(1), 62–80.

Janouchová, E. & Kučerová, A. 2013: Competitive Comparison of Optimal Designs of Experiments for Sampling-based Sensitivity Analysis. Accepted for publication in *Computers & Structures*, eprint: arXiv:1201.0942.

Marek, P. & Brozzetti, J. & Guštar, M. & Tikalsky, P. editors. 2003 : *Probabilistic assessment of structures using Monte Carlo simulation*, Institute of Theoretical and Applied Mechanics, Academy of Sciences of the Czech Republic, Prague, second edition.

Matthies, H. G. & Keese, A. 2005: Galerkin methods for linear and nonlinear elliptic stochastic partial differential equations. *Computer Methods in Applied Mechanics and Engineering* 194(12–16), 1295–1331.

Matthies, H. G. 2007: Uncertainty quantification with stochastic finite elements. In Erwin Stein, René de Borst, and Thomas J. R. Hughes, editors, *Encyclopaedia of Computational Mechanics*. John Wiley & Sons, Chichester.

Stefanou, G. 2009: The stochastic finite element method: Past, present and future. *Computer Methods in Applied Mechanics and Engineering* 198(9–12), 1031–1051.

Xiu, D. & Karniadakis, G. E. 2002: The Wiener–Askey Polynomial Chaos for Stochastic Differential Equations. *SIAM Journal on Scientific Computing* 24(2), 619–644.

Xiu, D. 2009: Fast Numerical Methods for Stochastic Computations: A Review. *Communications in Computational Physics* 5(2–4), 242–272.